Estimating Precipitation in the Central Cascades of Washington

P. S. HAYES, L. A. RASMUSSEN, AND H. CONWAY

Department of Earth and Space Sciences, University of Washington, Seattle, Washington

(Manuscript received 3 May 2001, in final form 7 December 2001)

ABSTRACT

Precipitation in the central Cascades of Washington correlates well over 1966–96 with wind and moisture in twice-daily upper-air soundings at a radiosonde station near the Pacific coast, 225 km away. A simple model estimates precipitation by using the component of the wind roughly normal to the north–south range of the Cascade Mountains, which it raises to a power and scales by the relative humidity. Values at 850 mb are taken as an index of the total moisture flux. Thresholds are imposed for the wind component and the relative humidity to reduce the likelihood of estimating precipitation from weak onshore flow on dry days. A split-sample analysis indicates that the model parameters are highly robust against sampling error. This moisture flux model estimates precipitation over 5-day periods with the coefficient of determination $r^2 \approx 0.55$, which increases for precipitation aggregated over 30-day periods to 0.75 and decreases to 0.30 for daily precipitation. Results over a 4-month period in the winter of 1996/97 were comparable to those from an advanced mesoscale precipitation model. The model estimates water-year (October–September) runoff for the period 1966–96 from two drainage basins in the region with $r^2 \approx 0.8$, and on 1 May forecasts subsequent May–September runoff with $r^2 \approx 0.4$.

1. Introduction

Determining the mesoscale distribution of precipitation is important on a daily basis for flood and avalanche forecasting, and over longer periods for water resource management, including hydroelectric power generation, fisheries, irrigation, and municipal water supply. Although advances in computing technology have made high-resolution numerical precipitation models increasingly accessible, simple models may provide adequate precipitation estimates for many purposes. Numerous studies have demonstrated strong correlations between large-scale atmospheric variables and observed precipitation at the surface (Cayan and Roads 1984; Wilby and Wigley 2000; Widmann and Bretherton 2000). Rasmussen et al. (2001) describe a model that estimates precipitation on the Olympic peninsula of western Washington from 850-mb wind and moisture at a nearby radiosonde station. Here we test that model at 14 stations and over two drainage basins in the central Cascades of Washington to determine how the model does for stations at greater distances from the radiosonde, at stations of low and high elevation, as well as how well moisture flux at the radiosonde station correlates to basin runoff. In addition, we test the model along the linear Cascades to investigate whether the critical direction is primarily from the direction perpendicular to the orientation of the range, as in the Sierra Nevada (Pandey et al. 1999), or the direction of greatest moisture transport, as for the cone-shaped Olympic Peninsula.

The model has both advantages and shortcomings. It is very economical of computer resources. It takes as its few inputs upper-air variables that have been routinely measured globally since 1948. These data are meticulously checked and systematically archived in the National Centers for Environmental Prediction (NCEP) reanalysis database (Kalnay et al. 1996), as well as being produced by general circulation models. The model is limited to use for stations with an existing precipitation record, because the record is needed to calibrate two station-specific model parameters. An additional shortcoming is that the variance of estimated precipitation is smaller than observed. Applications needing precipitation estimates over periods of several days or more might find the output satisfactory: for instance, estimation of the water content of mountain snowpacks and of glacier accumulation, or extension of a precipitation record that spans only a part of the radiosonde era.

a. Previous work

Numerous studies have investigated the distribution of precipitation (Schermerhorn 1967; Rasmussen and Tangborn 1976; Speers 1986) and the interaction of storms with the Cascade Mountains (Hobbs et al. 1971, 1975). Mass (1981, 1982) analyzed the influence on precipitation in western Washington from topographically forced convergence and diurnal variations in cir-

Corresponding author address: L. A. Rasmussen, Department of Earth and Space Sciences, University of Washington, Box 351310, Seattle, WA 98195.
E-mail: lar@geophys.washington.edu

culation. Chien and Mass (1997b) used the nonhydrostatic version 5 of the Pennsylvania State University (PSU)–National Center for Atmospheric Research (NCAR) mesoscale model (MM5) to investigate the impact of the Olympic and Cascade Mountains on the development of a Puget Sound convergence zone. Interactions of individual frontal systems with the complex terrain of the Pacific Northwest were modeled with MM5 in several studies (Colle and Mass 1996, 2000; Colle et al. 1999a; Chien and Mass 1997a; Steenburgh and Mass 1996). Colle et al. (1999b) evaluated MM5 at approximately 150 stations across the Pacific Northwest from 9 December 1996 to 30 April 1997. They found a relative error $(P^* - P)/P$ for individual stations in the Cascades for the 143-day period exceeding +0.40 ''along many of the steep windward slopes.'' The measured precipitation is P, and the model estimate is P^*. Barros and Lettenmaier (1993) calibrated their three-dimensional model with observed precipitation over the Olympic Peninsula for 1967, then compared estimated precipitation for the period 1968–74 with observed station precipitation and snow course amounts as well as average precipitation over three drainage basins: relative errors for winter totals were +0.36 for the Hoh, +0.25 for the Quinault, and −0.11 for the Elwha River basins. Wilson et al. (1992) describe a stochastic model for estimating daily precipitation from weather states, which are defined in terms of large-scale surface pressure; 850-, 700-, and 500-mb geopotential heights; and 850-mb wind. The model estimated precipitation over 1964–88 at Cedar Lake with relative errors of −0.11 for January–March, −0.04 for April–June, +0.06 for July–September, and −0.11 for October–December [P^* and P values taken from Wilson et al. (1992, their Table 6)]. Relative errors at Stampede Pass for the four seasons were +0.03, +0.14, +0.15, and −0.03.

From a qualitative correlation between water vapor flux and observed daily precipitation in California, Kim (1997) suggests that ''the amount of precipitation within the region may be directly related to the large-scale moisture flux field.'' Pandey et al. (1999) found that winter precipitation in California correlates strongly with 700-mb moisture flux from 240°, the direction normal to the mean trend of the Sierra Nevada. Rasmussen et al. (2001) demonstrated that daily precipitation at Forks, a lowland station on the west side of the Olympic Peninsula, correlates well with the 850-mb moisture flux from 238° at a nearby radiosonde station; elsewhere on the peninsula, precipitation correlates better with the moisture flux from the southwest than in the local upslope direction.

b. Data sources

We examine the correlation between precipitation measured daily at 10 National Weather Service (NWS) stations in the central Cascades and twice-daily measurements of 850-mb wind and humidity in the Quillayute radiosonde (Fig. 1) from 1 August 1966 through 31 December 1996. Station elevations (Table 1) differ from the contours in Fig. 1 because smoothed topography exerts more control over precipitation than actual topography (Schermerhorn 1967; Rasmussen and Tangborn 1976; Speers 1986). The NWS precipitation records, published monthly by state in the National Oceanic and Atmospheric Administrations *Climatological Data* summaries (NOAA 1966–96), included nine cooperative observer sites and the Weather Service Contract Meteorological Observatory at Stampede Pass. The Quillayute radiosonde observations are archived by the National Climatic Data Center in Asheville, North Carolina, and are reformatted and distributed by the Data Support Section of NCAR in Boulder, Colorado.

Precipitation measured hourly by heated tipping bucket gauges during the wet season between 1984 and 1996 (Table 1), and summed to get daily totals, at four Northwest Avalanche Center (NWAC) telemetry sites was also compared with radiosonde observations. The correlation between Quillayute 850-mb winds and winds in the Cascades was examined with measurements from an unheated anemometer at the NWAC site on the summit of Denny Mountain, adjacent to Snoqualmie Pass (Fig. 1).

From January 1948 until the radiosonde station moved to Quillayute in 1966, it was at a location about 50 km to the north and 10 km to the west. Radiosonde soundings usually occur at 0400 and 1600 local standard time (LST), their universal time coordinates being, respectively, 1200 UTC of the current day and 0000 UTC of the following day. Occasional soundings at times an hour or so different were interpolated linearly to these times during construction of the database used in this study. Precipitation observations at the NWS stations are at 0000 or about 0800 or 1700 LST for the previous 24-h period.

2. Climatology

In western Washington, Puget Sound separates the cone-shaped Olympic Mountains from the Cascade Mountains, which are aligned north to south about 225 km east of the Pacific coast (Fig. 1). A chain of volcanic peaks, with elevations to 4400 m (Mt. Rainier), extend from British Columbia south into Oregon, west of the Cascade crest which has peaks as high as 3000 m and gaps as low as 1000 m.

The Cascade range strongly influences the distribution of precipitation over the region, with mean annual amounts ranging from approximately 900 mm in the Puget Sound lowlands west of the range, to 1400–3000 mm along the crest, and 200–500 mm east of the mountains. There is substantial variability within the Cascades as well. Precipitation at stations near and west of the crest of the central Cascades, ranges (Table 1) from 0.67 to 1.44 times that at Longmire which is at 842 m on the south side of Mt. Rainier.

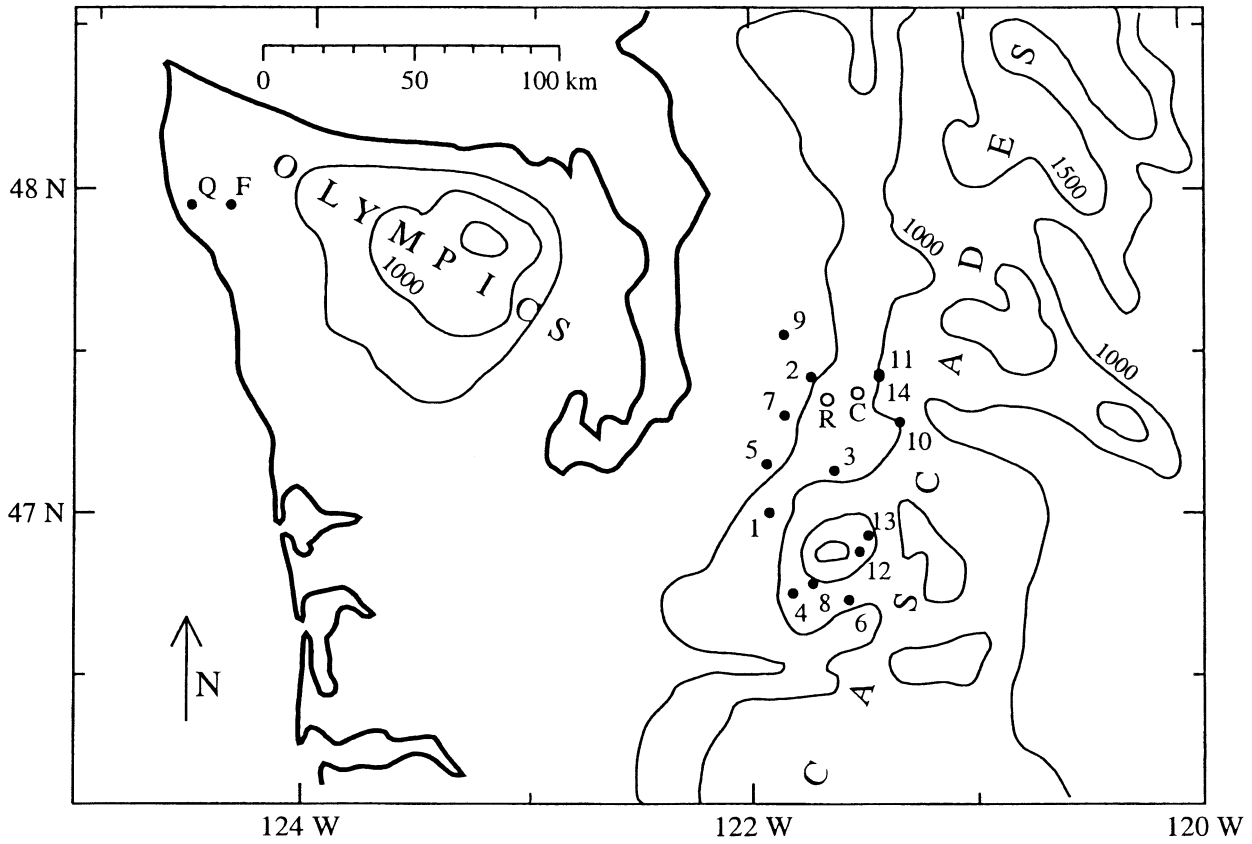

FIG. 1. Western Washington with weather stations (solid circles with location numbers; see Table 1): Quillayute radiosonde (Q); Forks (F); and streamflow stations Cedar River near Cedar Falls (C), and Rex River (R). Alpental (station 11) is on Denny Mountain, which is adjacent to Snoqualmie Pass (station 14). Coastline (heavy line) and topography (contour interval 500 m) are averaged over about 15 km. Puget Sound is the large indentation to the east of the Olympic Peninsula.

Most precipitation in the Pacific Northwest is produced by extratropical cyclones moving inland from the Pacific Ocean. The strong seasonal variation of precipitation, shown for Longmire in Table 2, has a winter maximum resulting from the greater duration, intensity, and frequency of cyclones during winter than summer. Convective storms, typical of midlatitude continental regions, are uncommon even in summer. Longmire precipitation is well correlated with other stations in the central Cascades (Table 3).

TABLE 1. Weather stations. Mean precipitation $\overline{P}$ is relative to Longmire. Elevations are meters above National Geodetic Vertical Datum of 1929.

Station No.*	Station name	Lat (N)	Lon (W)	Elevation	Period	$\overline{P}$
1	Carbon River	47.00	121.92	529	1966–73	0.87
2	Cedar Lake	47.42	121.73	476	1966–96	1.20
3	Greenwater	47.13	121.63	527	1966–81	0.64
4	Longmire	46.75	121.82	842	1966–96	1.00
5	Mud Mountain Dam	47.15	121.93	399	1966–96	0.71
6	Ohanapecosh	46.73	121.57	595	1966–96	0.92
7	Palmer	47.30	121.85	280	1966–96	1.06
8	Paradise	46.78	121.73	1655	1966–96	1.44
9	Snoqualmie Falls	47.55	121.85	134	1966–96	0.75
10	Stampede Pass	47.28	121.33	1207	1966–94	1.07
11	Alpental	47.43	121.42	976	1984–96	1.19
12	Chinook Pass	46.88	121.52	1683	1988–96	0.73
13	Crystal Mountain	46.93	121.48	1341	1989–96	0.67
14	Snoqualmie Pass	47.42	121.42	921	1989–96	1.21

* As shown in Fig. 1.

TABLE 2. Estimation of Longmire precipitation. Mean observed 5-day precipitation $\bar{P}$, its standard deviation σ, and statistics [minimum (min), maximum (max), mean bias error (mbe), and root-mean-square difference (rmsd)] of residuals $P^* - P$, all in millimeters for 1966–96 over indicated number n of 5-day periods when P reported.

Month	n	$\bar{P}$	σ	Min	Max	Mbe	Rmsd
Jan	190	52	74	−138	79	−3	35
Feb	173	40	61	−211	58	−1	30
Mar	191	28	38	−66	59	2	18
Apr	184	24	33	−96	42	0	16
May	185	17	24	−45	40	−1	14
Jun	186	16	27	−88	39	−4	18
Jul	188	7	14	−38	27	1	11
Aug	194	9	18	−105	37	1	15
Sep	185	18	30	−72	31	−3	17
Oct	194	29	42	−107	55	3	23
Nov	183	52	66	−119	69	−4	29
Dec	185	51	68	−160	60	−4	31

Rasmussen et al. (2001, their Fig. 4) observe that the mean southwesterly component of the 850-mb wind at Quillayute is much stronger in winter than in summer, and is stronger on wet days than on dry days. Southwesterly winds at the summit of Denny Mountain, adjacent to Snoqualmie Pass on the Cascade crest, correlate well with Quillayute 850-mb southwesterly winds for wet periods during the wet season (Fig. 2). Although the difference in mean directions is consistent with cyclonic curvature, complex wind patterns in Snoqualmie Pass likely influence the wind direction at Denny Mountain. With surface low pressure west of the Cascade crest and south-to-southwesterly winds at 850 mb at Quillayute, for instance, east winds channeled through Snoqualmie Pass result in southeast-to-east winds at Denny Mountain. Channeling through Snoqualmie Pass is also indicated by more westerly winds at Denny Mountain than at Quillayute.

3. Estimating precipitation

a. Flux model

Following Rasmussen et al. (2001), precipitation is estimated from twice-daily measurements of the 850-mb wind and humidity in the Quillayute radiosonde by the relation

$$P^* = \alpha U^M \mathrm{RH}, \tag{1}$$

in which

$$U = \begin{cases} |\mathbf{V}_{850}| \cos(\phi_{850} - \phi') & (U > U_{\min} \text{ and } \mathrm{RH} > \mathrm{RH}_{\min}) \\ 0 & (\text{otherwise}). \end{cases} \tag{2}$$

Here ϕ_{850} is the direction and $|\mathbf{V}_{850}|$ the speed of the 850-mb wind, and $0 \le \mathrm{RH} \le 1$ is the relative humidity. Yield factor α and critical direction ϕ' are determined empirically for each station (Fig. 3) to give the best fit to observed precipitation over successive 5-day periods during the period of record (Table 1). Constraints $U_{\min} = 2$ m s^{-1} and $\mathrm{RH}_{\min} = 0.64$ are imposed to avoid estimating precipitation on occasions of weak onshore flow. The exponent $M = 1.4$ is adopted from Rasmussen et al. (2001) for all stations, although results are not appreciably better than if $M = 1$ had been used; if M is set to another value, however, the optimum value of α will change accordingly to preserve the approximate value of αU^M.

Values of P^* from the individual soundings are added to estimate total precipitation under the assumption that each sounding represents conditions over the 12-h period centered at the time of the sounding. Precipitation observations made daily at 0000 or about 0800 or 1700 LST were phased approximately with the 0000 and 1200 UTC radiosonde data by using the two soundings immediately prior to the observation. Dry conditions are indicated by the model when $U = 0$ [Eq. (2)].

The quantity U^M RH at 850 mb is used as an approximation of the divergence of the moisture flux, which corresponds directly (when the divergence is negative) to the amount of moisture removed from the air. This is done first on the assumption that when the flow is from the sector of ϕ', the negative divergence correlates strongly with U^M RH. Second is the assumption that U^M RH, which is strictly a pseudoflux, is a better indicator of precipitation potential than the true moisture flux $U^M e$, in which e is the vapor pressure or specific humidity, because precipitation is a saturation phenomenon. Pandey et al. (1999) found that the moisture flux at Oakland, California, reached a maximum near 800 mb. This level carries more moisture than higher levels, yet is high enough to sample free-air conditions, and its wind is strongly correlated with winds at higher levels. The third assumption is that the total flux in the vertical column correlates well with that at 850 mb, which is used here because it is a standard level, routinely reported and archived.

Orographically induced vertical velocities, which are powerful producers of precipitation, are implicitly accounted for by the strength of U in the generally upslope direction. The critical direction ϕ', however, as will be discussed, reflects both topographic influences and the direction (Fig. 4) of strong moisture advection. The slight superiority of the RH formulation in estimating precipitation on the Olympic Peninsula (as well as of using $M = 1.4$ instead of unity) is shown in Table 4 of Rasmussen et al. (2001).

TABLE 3. Correlation of monthly precipitation at other stations with Longmire's precipitation. Percent values are given only for months in which both stations reported measurements in at least 15 years.

Station	Jan	Feb	Mar	Apr	May	Jun	Jul	Aug	Sep	Oct	Nov	Dec
Carbon River						91	81	88	82	96		
Cedar Lake	91	90	86	88	90	90	87	85	90	87	89	86
Greenwater	95	93	87	86	93	84	80	91	90	95	90	89
Mud Mountain Dam	94	83	75	75	89	88	90	89	85	90	87	84
Ohanapecosh	93	88	93	90	87	83	92	93	96	98	96	89
Palmer	87	88	85	86	86	91	86	85	89	85	90	83
Paradise	91	92	79	90	85	90	89	84	96	96	94	92
Snoqualmie Falls	91	85	78	85	84	79	83	90	85	87	92	79
Stampede Pass	89	88	86	83	85	84	84	93	89	93	93	85

b. Results

The performance of the model was measured by the root-mean-square difference (rmsd) between the model estimates P^* and observed precipitation P and by the coefficient of determination

$$r^2 = 1 - \left(\frac{\text{rmsd}}{\sigma}\right)^2, \tag{3}$$

in which σ is the standard deviation of P.

Over the entire 30-yr period 1966–96, the model estimated 5-day precipitation for Longmire with coefficient of determination $r^2 = 0.60$ and rmsd = 22.8 mm. Longmire is used here as an indicator station because 1) it has a better precipitation correlation with other stations in the central Cascades (Table 3) than any other station has; 2) it has a more complete precipitation record than the Paradise or Stampede Pass stations, the other two high-elevation sites; and 3) it is at an elevation that is near, but usually below, the snow level, thus

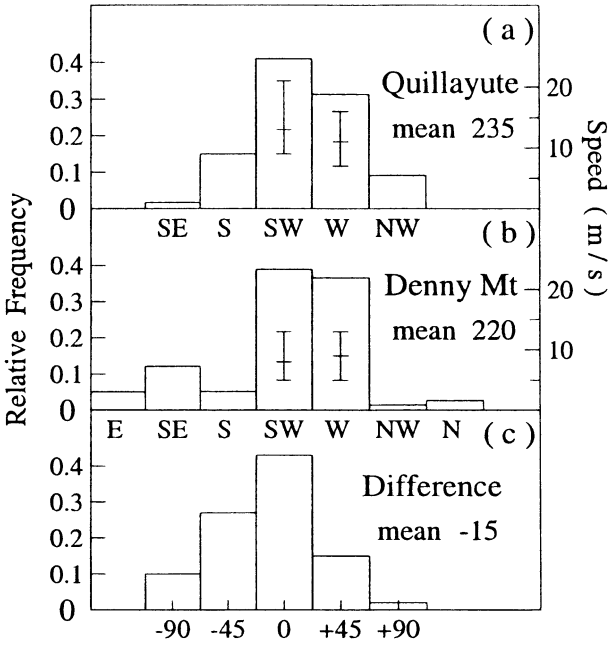

FIG. 2. Frequency distributions of winds in 702 soundings over the wet seasons 1984–96, during which wind speed at both Quillayute and Denny Mountain exceeded 2 m s^{-1}, and Denny Mountain received more than 2.5 mm of precipitation in the 6 h after the sounding. (a) Quillayute at 850 mb (≈1450 m). (b) Denny Mountain (1999 m) 3 h after the time of the sounding. (c) Denny Mountain minus Quillayute. Octants with less than 0.02 of the distribution are not shown. The error bars for the W and SW octants indicate roughly the bottom sixth, the median, and the top sixth of the frequency distribution of the speed (the points that the mean minus one standard deviation, the mean, and the mean plus one standard deviation cut off in a normal distribution). Denny Mountain is near Alpental (Fig. 1. station 11).

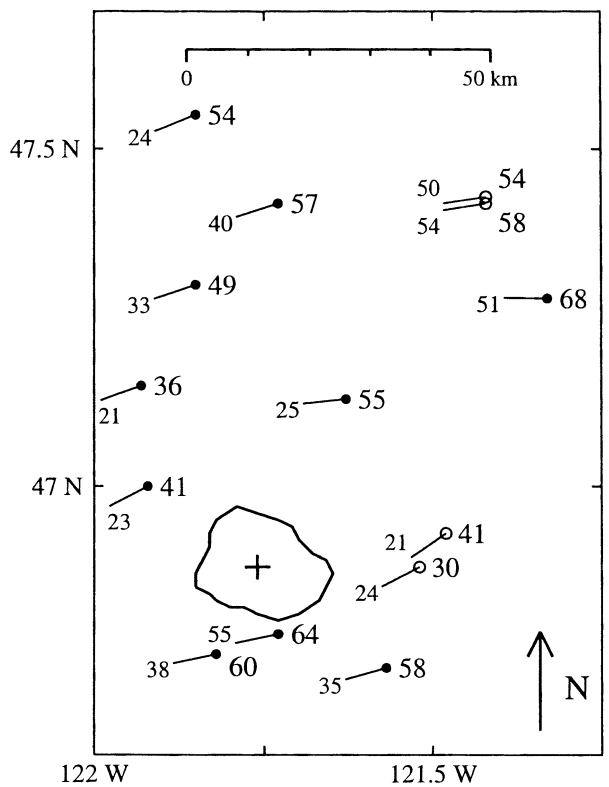

FIG. 3. Model results for 5-day aggregation periods. The 14 stations are the same as shown in Fig. 1. The staff shows the critical direction ϕ' of the Quillayute 850-mb wind, the small number at the end of the staff is the yield factor α (×100), the large number is percent r^2, solid circles are NWS stations, and open circles are NWAC stations. Also shown is a 2000-m contour around Mt. Rainier, the summit of which (4400 m) is indicated by the cross.

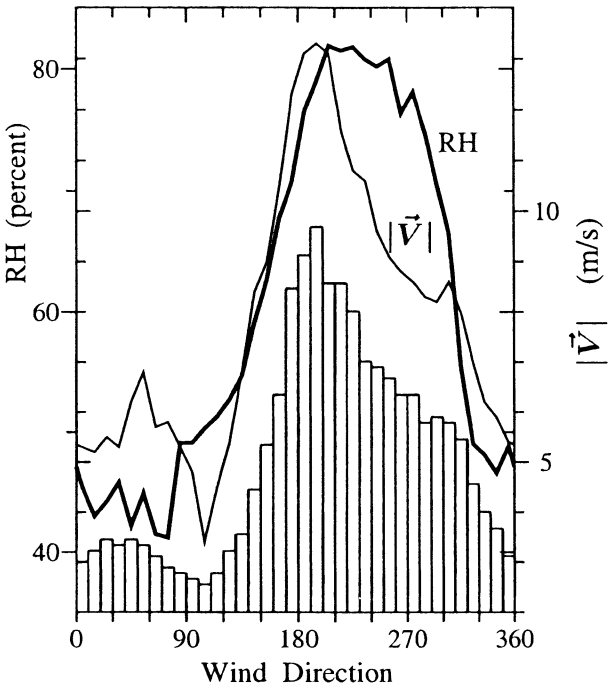

FIG. 4. Frequency distribution of Oct–May wind direction, along with mean speed $|\mathbf{V}|$ and RH at 850 mb in Quillayute radiosonde over the period 1966–96.

avoiding precipitation measurement errors associated with snowfall. Statistics by month of estimates of the 5-day precipitation are shown in Table 2, the distribution of rmsd roughly following the seasonal distribution of precipitation. Although the absolute rmsd is greatest during winter, when the mean precipitation and its variance are also large, the relative rmsd (the ratio of the rmsd to σ) is smaller in winter than in summer.

The 30-yr Longmire record contains 100 precipitation streaks with greater than 50 mm day^{-1}, of which 85 lasted for one day, 12 for 2 days, 2 for 3 days, and 1 for 4 days. Residuals by precipitation amount (Table 4) indicate that the model fails to capture extreme events, most of which occur in November through February, which are the months with the largest rmsd errors for 5-day estimates and with the greatest precipitation (Table 2). The rmsd errors are even larger for 1-day precipitation estimates. When the model results are summed over 30-day periods, r^2 for Longmire increases to 0.78, and when summed only daily it decreases to 0.34 (Table 5).

For the other nine NWS stations, r^2 also increases substantially as the aggregation period lengthens from 1 to 30 days (Table 5). Values of r^2, which range from 0.14 at Mud Mountain Dam to 0.47 at Stampede Pass for daily precipitation, increase to 0.45 and 0.83 for 30-day amounts at those two stations. The greatest increase generally occurs between 1- and 2-day aggregations (not shown in Table 5), with the rate of increase generally diminishing through 30 days. This is most likely related to the decreasing influence of observation-time phasing problems as the aggregation period lengthens, as well as to the cancelation of errors from underestimating precipitation for some days in the period and overestimat-

TABLE 4. Distribution of statistics [minimum (min), maximum (max), mean bias error (mbe), and root-mean-square difference (rmsd)] of residuals $P^* - P$. Results are for 5-day precipitation P at Longmire over 1966–96. All quantities are in millimeters. There are n occurrences in each interval.

P	n	Min	Max	Mbe	Rmsd
≤0.1	322	0	55	4	8
1–5	429	−5	48	7	12
6–15	373	−15	66	5	14
16–30	380	−30	55	2	16
31–50	312	−39	74	−1	21
51–100	307	−89	79	−11	30
>100	115	−211	40	−51	65

TABLE 5. Estimation of 5-day precipitation. Critical direction ϕ' is 850-mb wind in Quillayute radiosonde correlating best with 5-day precipitation and α is the yield factor [Eq. (1)]. Standard deviation (σ), mean bias error (mbe), and root-mean-square difference (rmsd) are all in millimeters. Values of r^2 are from model optimized for 5 days and tested for aggregation periods of 1, 5, and 30 days. Results for the last four stations are for winter only and for a shorter period than the others (Table 1).

	For 5-day period					r^2		
Station	ϕ'	α	σ	Mbe	Rmsd	1 day	5 day	30 day
Carbon River	242°	0.233	22.6	−2.9	17.4	0.16	0.41	0.51
Cedar Lake	252°	0.399	39.1	−3.3	25.5	0.32	0.57	0.76
Greenwater	264°	0.252	22.9	−1.0	15.3	0.29	0.55	0.79
Longmire	258°	0.378	35.9	−1.0	22.8	0.34	0.60	0.78
Mud Mountain Dam	250°	0.207	22.3	−3.5	17.8	0.14	0.36	0.45
Ohanapecosh	254°	0.350	37.2	0.4	24.0	0.33	0.58	0.78
Palmer	251°	0.329	33.0	−4.1	23.6	0.23	0.49	0.67
Paradise	258°	0.546	50.1	−1.2	30.2	0.37	0.64	0.80
Snoqualmie Falls	248°	0.242	26.4	−1.4	17.8	0.28	0.54	0.77
Stampede Pass	271°	0.509	38.6	−0.8	21.9	0.47	0.68	0.83
Alpental	261°	0.500	56.0	0.2	37.8	0.30	0.54	0.65
Chinook Pass	243°	0.239	33.7	−2.3	28.2	0.14	0.30	0.38
Crystal Mountain	236°	0.212	34.5	−0.4	26.4	0.24	0.41	0.53
Snoqualmie Pass	261°	0.535	60.0	1.9	39.0	0.37	0.58	0.46

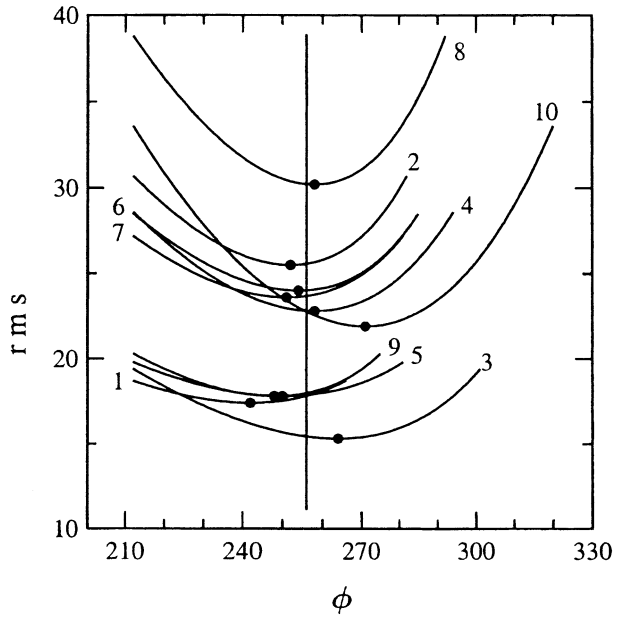

FIG. 5. Sensitivity of rms error to critical direction ϕ' of the Quillayute 850-mb wind for the 10 NWS stations (Table 1). The single direction best fitting the 10 stations overall (vertical line) is $\overline{\phi}' = 256°$.

ing it for others. When the model is applied over winter to the four NWAC stations (the last four in Table 5), r^2 for 5-day precipitation ranges from 0.30 at Chinook Pass to 0.58 at Snoqualmie Pass. Low r^2 at Chinook Pass may be related to several factors, including substantial missing data during midwinter when propane used to heat the gauge runs out. This results in there being disproportionately more observations in spring when precipitation from showers is more common.

When applied to Forks over 1948–96 (Rasmussen et al. 2001), the model estimated precipitation with $r^2 = 0.73$ for 5-day precipitation and $r^2 = 0.84$ for 30-day amounts. The model yields slightly lower r^2 for 5-day amounts than that at Forks for stations at increasing elevation in the Cascades: 0.60 at 842 m (Longmire), 0.68 at 1207 m (Stampede Pass), and 0.64 at 1655 m (Paradise). The variability of r^2 in the central Cascades (Table 5) may be due in part to the complex topography of the region resulting in a complicated relationship between moisture flux at a particular site and the critical direction ϕ' of the Quillayute 850-mb wind. Variation of ϕ' associated with the cone shape of Mt. Rainier, similar to that found by Rasmussen et al. (2001) for the Olympic Peninsula, may be superimposed on the regional value, which is indicated by ϕ' to be more southerly to the east of the cone (Fig. 3). Speers (1986) found that Mt. Rainier had a significant shadowing effect on precipitation at surrounding stations and that the effect varied with wind direction. For the 14 central Cascade stations, ϕ' ranges from 236° to 271° (Table 5), but errors are relatively insensitive to it (Fig. 5). Using the best-fitting single value $\overline{\phi}' = 256°$ yields negligible increases in rmsd at individual NWS stations, except for the two stations (Table 5) with ϕ' appreciably different from 256° [0.5 mm (5 days)$^{-1}$ at Carbon River, and 1.5 mm (5 days)$^{-1}$ at Stampede Pass].

In the California Sierra Nevada, Pandey et al. (1999) observed that the heaviest precipitation was associated with 700-mb winds from 220°–240°, roughly perpendicular to the orientation of the range. In the central Cascades, although the ϕ' are more westerly than in the Sierra Nevada, with the single best ϕ' being 256° and about 240°, respectively, both are roughly perpendicular to the overall trend of the range. In contrast, $\phi' = 238°$ for Forks reflects the predominant transport of moisture from the southwest as well as the upslope direction. For 19 other stations around the periphery of the cone-shaped Olympic Mountains (Rasmussen et al. 2001), the critical direction ϕ' of the Quillayute 850-mb wind varies from 210° to 257°, with directions for stations along the eastern side of the peninsula more southerly and those along the northwesterly edge more westerly than for Forks. This variation primarily reflects moisture availability, and only secondarily the effect of the topography, because flow can go around the Olympic Mountains. In contrast, because air cannot flow around the long, linear Cascades, the upslope effect normal to the trend of the range overrides the importance of the direction of maximum moisture flux.

c. Model residuals

Many sources of error afflict the flux model. Because it only crudely represents physical processes, it does not directly account for vertical velocity or static stability, both important to precipitation. Atmospheric conditions are coarsely sampled twice daily at a single level from one radiosonde station. This temporally and spatially coarse sampling may miss rapidly moving meteorological events as well as small-scale phenomena, such as convective cells or rainbands embedded in synoptic systems (Hobbs 1978). Pandey et al. (2000) partially resolve this by driving their model for the Sierra Nevada with separate upper-air profiles from three radiosonde stations and averaging the precipitation estimates from each.

Numerous errors and inhomogeneities exist in the radiosonde moisture record. Rasmussen et al. (2001) demonstrated a significant redistribution of soundings within the 81%–90% and 91%–100% RH intervals in the Quillayute radiosonde (their Fig. 6) associated with the transition to VIZ hygristors (VIZ Meteorological Systems Group, Sippican, Inc.) in 1963 (Schwartz and Wade 1993). Although the central Cascades study avoids that instrument transition by starting in 1966, from 1963 until the instrument housing was replaced in 1972 solar radiation fell directly on the carbon hygristor, which caused errors (Gaffen et al. 1991; Zhai and Eskridge 1996) in daytime RH values (Fig. 6). In 1980 and again in 1988–89, new model VIZ hygristors were deployed

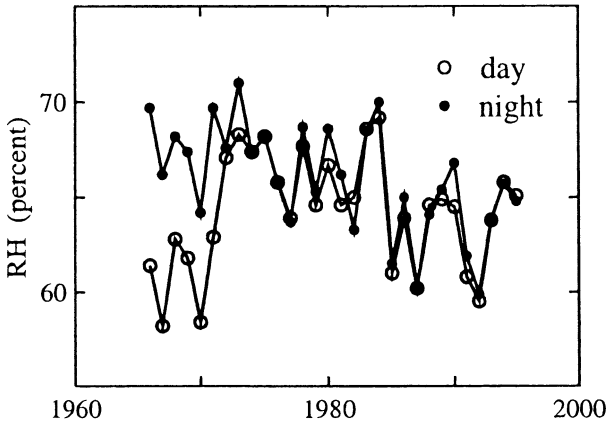

FIG. 6. Mean annual daytime and nighttime RH (%) at 850 mb in Quillayute radiosonde over 1966–96.

at Quillayute with response characteristics different from previous sensors (Elliott and Gaffen 1991). The instrument's actual response curve departed from the VIZ conversion algorithm at about 70% RH and reached a maximum departure of 3%–4% near 90% RH (Wade and Schwartz 1993). Between 1988 and 1989, when the NWS changed the parallel resistor in the circuit, and 1993, when the conversion algorithm was corrected, RH values near saturation were being reported too low by 3%, with the effect decreasing and becoming negligible at 60% (Elliott et al. 1998; Wade and Schwartz 1993). There are also errors associated with recording methods. In February 1983, for example, most of the recorded 850-mb RH at Quillayute was between 48% and 52%, which is not consistent with reported temperature and dewpoint. Although we have found similar recording discrepancies in other months at Quillayute, we do not know how prevalent they are or what other periods might be afflicted.

Precipitation measurement is also afflicted by many error sources, especially at low temperatures. NWS cooperative observer stations measure precipitation with standard 8-in. diameter gauges. Although most of them are unshielded, some NWS gauges have been equipped with Alter wind shields, which can increase the rainfall catch by several percent and the solid precipitation catch by tens of percent (Yang et al. 1998). This has resulted in temporal inhomogeneities at some stations as well as possible spatial interpretation errors. Gauge catch decreases with increasing wind speed, resulting in an undercatch of 3%–10% for rainfall, and up to 50% or more for snowfall (Groisman and Legates 1994). Systematic errors occur due to wetting gauge surfaces at the onset of precipitation, evaporative losses, especially with heated gauges, and the treatment of trace precipitation as zero. In complex terrain, precipitation may vary strongly over short distances. For example, Sinclair et al. (1997) document 24-h precipitation measurements of 125 and 315 mm at gauges 2 km apart in New Zealand.

Imperfect time phasing of precipitation observations with radiosonde soundings degrades model results, more severely the shorter the aggregation period. On the assumption that each sounding represents conditions over the 12-h period centered on its time, two successive soundings would represent a 24-h period ending at either 1000 or 2200 LST, depending on which two soundings are paired, but precipitation observations at NWS stations do not occur at either of those times. For stations with evening observations, the model attempts to minimize the phasing error by using radiosondes at 0400 and 1600 LST on the current day; for morning observations, it uses those at 1600 LST on the previous day and 0400 LST on the current day.

The possible lag between conditions in the Cascades and at the Quillayute radiosonde station was investigated by using hourly precipitation over the winters of 1984–96 at the NWAC Alpental station near Snoqualmie Pass (Fig. 1). Total precipitation over the 24-h period centered on two successive radiosondes does not correlate as well with the moisture flux as does the 24-h period beginning 3h later, which indicates a 3-h lag from the coast to the Cascades. That is, the 24-h period with radiosondes occurring 3 and 15 h into the period correlates better than the one with them occurring 6 and 18 h into the period.

d. Model stability

Model parameters ϕ' and α are very stable. The Longmire record was divided into halves, each spanning the entire period of record, to test whether the results were heavily influenced by sampling error. When the flux model was calibrated for Longmire on only even-numbered 5-day periods (2, 4, . . . , 2238), ϕ' remained the same (258°) as for all 2238 periods, and α decreased from 0.378 to 0.360; when these values of ϕ' and α were applied to the odd-numbered 5-day periods (1, 3, . . . , 2237), r^2 increased from 0.60 to 0.61. When it was calibrated on only the odd-numbered periods, ϕ' increased to 259° and α increased to 0.391; when these values were applied to the even-numbered periods, r^2 decreased to 0.58. For the remaining nine NWS stations, these split-sample tests demonstrated similar model stability, with a maximum change over all stations of 3° in ϕ' and 0.04 in α, indicating that the values obtained for the model parameters were not heavily influenced by sampling error.

Some alternative forms of the flux model [Eq. (1)] were tested. When U alone was used, it did nearly as well as when RH was included, which might be because RH correlates well with 850-mb wind direction (Fig. 4). In addition, errors in RH (section 3c) likely degrade the results of the U–RH model. Using vapor pressure e in place of RH, as Pandey et al. (1999) did for the Sierra Nevada, yields slightly poorer results at all 10 NWS stations in the central Cascades than do either the U or U–RH models. This may be because precipitation is a

saturation phenomenon and relative humidity is a better indicator of saturation than vapor pressure, which varies strongly with temperature. The relative accuracy of these three alternative models was similar to results on the Olympic Peninsula (Rasmussen et al. 2001, their Table 4). The results given here for 30-day periods are obtained by applying model parameters ϕ' and α optimized for 5-day periods, but slightly better results would be obtained by reoptimizing for the 30-day periods, and similarly for any aggregation period. Enlarging the sector from which flux is calculated does not improve the results of the model optimized for 5-day periods. That is, when Eq. (2) is written

$$U = |\mathbf{V}_{850}| \cos[\psi(\phi_{850} - \phi')] \quad (4)$$

for $\psi < 1$, it has the effect of using ϕ_{850} from a wider interval around ϕ'. The optimum value at Longmire over the 30 years $\psi = 0.96$ gives $r^2 = 0.5984$ for 5-day aggregation, which is negligibly better than 0.5980 when using $\psi = 1$.

4. Comparison with MM5

MM5 was run twice daily from 9 December 1996 through 30 April 1997 to determine the accuracy of its precipitation estimates over a long cool season (Colle et al. 1999b, their Fig. 15). Precipitation values from 12–36-h forecasts were interpolated from the 12-km MM5 grid over Washington and Oregon to individual observation sites by using an inverse-distance Cressman method. These values were summed over the 143-day period to produce the estimate P^*, and in Colle et al. (1999b) were discussed in terms of the ratio to observed, P^*/P.

The flux model [Eqs. (1), (2)] was run for the same 1996/97 winter period using values of critical direction ϕ' and yield factor α determined at each station from the 1966–96 optimization for 5-day aggregation periods. The optimum ϕ' varies little between optimizations for the 1-day and 5-day aggregation periods, but α generally increases as the length of the period increases. Consequently, when summed over the 143-day period, the 5-day model underestimates the actual precipitation less than the model would if it were optimized over 1-day aggregation periods.

Results are expressed here (Table 6) by the relative error $(P^* - P)/P$. Because the MM5 estimates are given only for the entire 143-day aggregation period (Colle et al. 1999b), r^2 values cannot be calculated for individual stations. The algebraic mean (over the five stations for which both models give estimates) of the relative error is -0.06 for the flux model and $+0.11$ for MM5, with the flux model underestimating precipitation for all five stations, and MM5 underestimating for some and overestimating for others. Although five stations over only one period is a very small sample, Colle et al. (1999b) indicate that MM5 errors are persistent, with the model overestimating precipitation near volcanos and along steeper windward slopes of the Cascades and underestimating it within the Stampede gap. The five-station mean of the absolute value of the relative errors is 0.06 for the flux model and 0.25 for MM5. The flux model has the substantial advantage of having its model parameters calibrated for each station. Published precipitation data are not available during this period for Carbon River, Greenwater, and Stampede Pass. Values for Ohanapecosh and Paradise were not given by Colle et al. (1999b). The flux model was not compared with MM5 over daily or monthly periods because, other than precipitation estimates for individual storm totals (Colle and Mass 1996, 2000; Westrick and Mass 2001), there are no published MM5 precipitation data on these timescales.

TABLE 6. Comparison of flux model [Eqs. (1), (2)] and MM5. Flux model parameters α and ϕ' are for 5-day optimization (Table 5). Average daily precipitation $\bar{P}$ is in millimeters. Period is 9 Dec 1996–30 Apr 1997.

Station	$\bar{P}$	$(P^* - P)/P$	
		Flux model	MM5
Carbon River			+0.61
Cedar Lake	11.3	−0.02	−0.11
Greenwater			+0.20
Longmire	11.6	−0.15	+0.32
Mud Mountain Dam	5.8	−0.03	+0.35
Ohanapecosh	10.6	−0.11	
Palmer	10.2	−0.09	−0.25
Paradise	16.0	−0.14	
Snoqualmie Falls	7.9	−0.09	+0.23
Stampede Pass			−0.55

MM5 produces precipitation estimates on a fine-scale square grid, facilitating interpolation, whereas the flux model estimates are confined to the sparse array of existing observation locations. Another advantage of MM5 is that it normally operates in the prognostic mode, whereas the flux model would require prognostic wind and humidity data from some other model.

5. Estimating water-year runoff and predicting summer runoff

Moisture flux U^M RH in the direction $\overline{\phi}' = 256°$ at the radiosonde station yields a good estimate over 1966–96 of water-year (October–September) runoff from two drainage basins in the region (Fig. 1). Cedar River above Cedar Falls with a drainage area of 105 km^2 ranges in elevation from 476 m to about 1600 m, and nearby Rex River with an area of 35 km^2 ranges in elevation from 488 m to about 1400 m. Specific runoff over this period averages 2100 mm yr^{-1} for Cedar River and 2560 mm yr^{-1} for Rex River. The flux F [Eq. (1)] summed from $t_0 = 1$ October to some subsequent date t_w,

$$F(t_w) = \int_{t_0}^{t_w} U^M \mathrm{RH}\, dt, \quad (5)$$

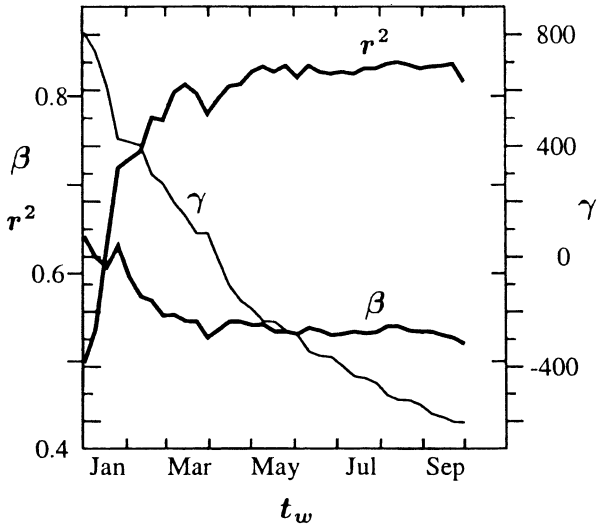

FIG. 7. Estimation of Oct–Sep streamflow R_y of the Cedar River near Cedar Falls. Regression coefficients β and γ [Eq. (6)] along with the coefficient of determination r^2 are shown as a function of the date t_w of the end of the season over which the total moisture flux $F(t_w)$ at 850 mb in the Quillayute radiosonde is used [Eq. (5)].

has a good linear relation with specific water-year runoff R_y:

$$R_y^* = \beta F(t_w) + \gamma. \quad (6)$$

When the flux is summed over the entire water year (t_w = 30 September), it gives $r^2 = 0.82$ for Cedar River and 0.77 for Rex River over the $n = 30$ water years 1967–96.

As noted by Rasmussen and Tangborn (1976), who used precipitation P at a lowland gauge near the drainage basin instead of F, the winter total P_w often afforded a slightly better estimate of water-year runoff R_y than did the water-year total P_y. This is also the case when F is used to estimate R_y for these two basins in the central Cascades. When F is summed over only September–April, the fits improve to $r^2 = 0.83$ for Cedar River and 0.81 for Rex River. Comparison of the linear fit [Eq. (6)] with the balance equation for the basin,

$$P_y = P_w + P_s = R_y + E_y + \Delta_y, \quad (7)$$

indicates that β corresponds to $P_w/F(t_w)$ and γ corresponds to $P_s - E_y - \Delta_y$. Here P_s is precipitation between t_w and 30 September, E_y is total water-year evapotranspiration, and Δ_y is the change over the year of storage of water in all forms: snow and ice, soil moisture, groundwater, etc. These two relatively low-elevation, unglacierized basins have no perennial snow or ice, so there is no contribution to Δ_y from those forms. The way β and γ vary for Cedar River, as t_w is taken to vary from the beginning of January to the end of September (Fig. 7), supports this interpretation. While β remains constant (within its standard error 0.05) after February, γ declines from being strongly positive to being strongly negative because of the decline of P_s as the period from t_w to 30 September is shortened. For t_w = 30 September, $P_s = 0$, so $\gamma = -604$ mm (Fig. 7) represents $-E_y$; for t_w = 30 April, $\gamma = -190$ mm indicates that $P_s = \gamma + E_y = 414$ mm for May–September precipitation. By comparison, mean May–September precipitation at Longmire is 404 mm. Results for Rex River are comparable.

As Tangborn and Rasmussen (1976) did with P_w for many basins in the Cascades, $F(t_w)$ can be used not only to estimate R_y but also as a means at the end of winter of forecasting the subsequent spring and summer runoff R_s. Because $R_y = R_w + R_s$ and the winter runoff R_w is known at time t_w, the forecast R_s^* of spring and summer runoff can be obtained from that of water-year runoff R_y^* by subtracting R_w from it. Over 1966–96, taking 30 April as t_w forecasts May–September R_s with $r^2 = 0.45$ for Cedar River and 0.36 for Rex River. Because R_w is known, the rmsd for forecasting R_s is the same as for R_y, but the r^2 [Eq. (3)] for R_s is lower than for R_y because σ is smaller for R_s than for R_y, owing to the large contribution of the variance of R_w to that of R_y.

For these basins, R_s is related to P_w because of the seasonal storage of snow falling before t_w and melting afterward. The storage produces mean values $\overline{R}_s/\overline{R}_y$ of 0.33 for Cedar River and 0.28 for Rex River, which is of slightly lower elevation, compared with $\overline{P}_s/\overline{P}_y$ of only about 0.16 in this region. The negligible influence of P_s on estimating R_y is presumably due to the large share of it that goes, during the warm growing season, to evapotranspiration instead of to runoff. This implies that much of $\overline{R}_s/\overline{R}_y$ comes from the part of $\overline{P}_w$ stored as snow until after t_w, not just the excess of $\overline{R}_s/\overline{R}_y$ above 0.16. Were there no storage of P_w as seasonal snow, it would not contribute to R_s, and evapotranspiration would cause R_s to be much less than P_s. Moreover, P_w and R_w would be ineffectual in forecasting R_s.

6. Summary and conclusions

A simple model for estimating precipitation from twice-daily measurements of 850-mb wind and relative humidity at a National Weather Service (NWS) radiosonde 225 km away near the Pacific coast is applied to stations in the central Cascades of Washington. For each station, its record of precipitation over 1966–96 is used to determine two model parameters empirically: critical direction ϕ' of the radiosonde 850-mb wind and yield factor α. Model estimates of precipitation, for periods ranging from 1 to 30 days, were compared with observed precipitation measured daily throughout the year for 10 NWS stations, and measured hourly during the cool season and summed to get daily totals for four Northwest Avalanche Center sites. Estimates for stations ranging in elevation from 134 to 1683 m in the central Cascades were comparable to estimates for stations near the radiosonde station on the Olympic Peninsula (Rasmussen et al. 2001).

The model underestimates extreme events and thus

does not produce a simulated time series of precipitation with high-frequency statistical characteristics comparable to those of actual precipitation. As pointed out by von Storch (1999), models such as the flux model produce estimated values with much smaller variance than that of observed values. It therefore would not be suitable for hydrologic models requiring precipitation series of high temporal resolution as input. Summing the estimates of precipitation from twice-daily upper-air measurements significantly improves the r^2 values as the resolution of the time series of estimates decreases from daily to longer periods. For periods of any length, however, it overestimates low-precipitation events and underestimates high-precipitation events. Using critical direction and yield factor determined empirically over 5-day periods gives estimates of 5-day precipitation with mean $r^2 = 0.55$ for the 10 NWS stations in the central Cascades, which increases to 0.75 for 30-day periods and decreases to 0.30 for daily precipitation. Although much of this improvement results from summing positive and negative errors, the effect of time phasing error (between radiosonde soundings and precipitation measurements) is also lessened over longer aggregation periods. Precipitation estimates improve slightly for any length of aggregation period when critical direction and yield factor are optimized over that length.

On the Olympic Peninsula, where it is possible to compare the predominant direction of moisture flux with the entire range of upslope directions (at precipitation stations entirely around the cone-shaped Olympic Mountains), the transport of moisture from the southwest quadrant overrides the importance of the local upslope direction (Rasmussen et al. 2001), with slight variations in critical direction for individual stations reflecting the effect of topography. In contrast, in the central Cascades the upslope direction perpendicular to the linear trend of the range is predominant over the direction of maximum moisture flux. However, in the vicinity of Mt. Rainier, a large cone-shaped volcano west of the Cascade crest, slight variations in critical direction ϕ' similar to those on the Olympic peninsula are superimposed on the regional value, with ϕ' being more southerly to the east of the cone (Fig. 3).

Flux model precipitation estimates from 9 December 1996 through 30 April 1997 were compared with 12-km MM5 estimates for five stations. The mean of the absolute value of the relative errors was 0.06 for the flux model and 0.25 for MM5, with the flux model underestimating precipitation for all stations and MM5 overestimating for some and underestimating for others. Although the sample size of this comparison is small, only one period and only five stations, the results are consistent with other results for both models. The flux model has a bias in overestimating low precipitation and underestimating high precipitation. The 12-km MM5 overestimates precipitation along steep windward slopes and near volcanos, and underestimates it in the Cascade gaps.

October–September runoff from two drainage basins in the region is estimated with $r^2 \approx 0.8$ when radiosonde observations for the entire year are used. Summer precipitation, owing to great loss to evapotranspiration during the warm growing season, contributes little to the annual runoff, so that r^2 is hardly affected by using only the October–April soundings. Using only those soundings to estimate the annual runoff, and subtracting the observed October–April runoff from it, enables forecasting on 1 May the subsequent May–September runoff. For these two drainage basins, May–September runoff is forecast with $r^2 \approx 0.4$.

The flux model would be suitable for providing low-resolution time series of precipitation in numerous instances of water resource management, such as estimating the water content of mountain snowpacks and of glacier accumulation. The model's performance would likely be comparable to that in the central Cascades in other climatic regions where most precipitation results from extratropical cyclones moving onshore.

Two unexplored lines of inquiry have suggested themselves. One is interpolating the two model parameters ϕ' and α at locations where precipitation stations do not exist. Another is reconsidering the use of only RH or only specific humidity in the flux formulation, and perhaps using instead an expression of moisture that combines both the effect of nearness to saturation and of the absolute amount of moisture present.

Acknowledgments. This work was partly supported by National Science Foundation Grant ATM-9530691 and NASA Grant 1215388. We are especially grateful for the comments of anonymous reviewers, which have led not only to an improved paper but also to greater insight on the part of the authors into the character and limitations of the model. We thank Ken Westrick for supplying us with MM5 bias scores for individual stations in the central Cascades.

REFERENCES

Barros, A. P., and D. P. Lettenmaier, 1993: Dynamic modeling of the spatial distribution of precipitation in remote mountainous areas. *Mon. Wea. Rev.,* **121,** 1195–1214.

Cayan, D. R., and J. O. Roads, 1984: Local relationships between United States west coast precipitation and monthly mean circulation parameters. *Mon. Wea. Rev.,* **112,** 1276–1282.

Chien, F.-C., and C. F. Mass, 1997a: Interaction of a warm-season frontal system with the coastal mountains of the western United States. Part I: Prefrontal onshore push, coastal ridging, and alongshore southerlies. *Mon. Wea. Rev.,* **125,** 1705–1729.

——, and ——, 1997b: Interaction of a warm-season frontal system with the coastal mountains of the western United States. Part II: Evolution of a Puget Sound convergence zone. *Mon. Wea. Rev.,* **125,** 1730–1752.

Colle, B. A., and C. F. Mass, 1996: An observational and modeling study of the interaction of low-level southwesterly flow with the Olympic Mountains during COAST IOP 4. *Mon. Wea. Rev.,* **124,** 2152–2175.

——, and ——, 2000: The 5–9 February 1996 flooding event over

the Pacific Northwest: Sensitivity studies and evaluation of the MM5 precipitation forecasts. *Mon. Wea. Rev.,* **128,** 593–617.
——, ——, and B. F. Smull, 1999a: An observational and numerical modeling study of a cold front interacting with the Olympic Mountains during COAST IOP 5. *Mon. Wea. Rev.,* **127,** 1310–1334.
——, K. J. Westrick, and C. F. Mass, 1999b: Evaluation of MM5 and Eta-10 precipitation forecasts over the Pacific Northwest during the cool season. *Wea. Forecasting,* **14,** 137–154.
Elliott, W. P., and D. J. Gaffen, 1991: On the utility of radiosonde humidity archives for climate studies. *Bull. Amer. Meteor. Soc.,* **72,** 1507–1520.
——, R. J. Ross, and B. Schwartz, 1998: Effects on climate records of changes in National Weather Service humidity processing procedures. *J. Climate,* **11,** 2424–2436.
Gaffen, D. J., T. P. Barnett, and W. P. Elliott, 1991: Space and time scales of global tropospheric moisture. *J. Climate,* **4,** 989–1008.
Groisman, P. V., and D. R. Legates, 1994: The accuracy of United States precipitation data. *Bull. Amer. Meteor. Soc.,* **75,** 215–227.
Hobbs, P. V., 1978: Organization and structure of clouds and precipitation on the mesoscale and microscale in cyclonic storms. *Rev. Geophys. Space Phys.,* **16,** 741–775.
——, and Coauthors, 1971: Studies of winter cyclonic storms over the Cascade Mountains (1970–71). Contributions from the Cloud Physics Group, Research Rep. 6, University of Washington, Seattle, WA, 306 pp.
——, R. A. Houze, and T. J. Matejka, 1975: The dynamical and microphysical structure of an occluded frontal system and its modification by orography. *J. Atmos. Sci.,* **32,** 1542–1562.
Kalnay, E., and Coauthors, 1996: The NCEP/NCAR 40-Year Reanalysis Project. *Bull. Amer. Meteor. Soc.,* **77,** 437–471.
Kim, J., 1997: Precipitation and snow budget over the southwestern United States during the 1994–1995 winter season in a mesoscale model simulation. *Water Resour. Res.,* **33,** 2831–2839.
Mass, C. F., 1981: Topographically forced convergence in western Washington. *Mon. Wea. Rev.,* **109,** 1335–1347.
——, 1982: The topographically forced diurnal circulation of western Washington state and their influence on precipitation. *Mon. Wea. Rev.,* **110,** 8–21.
NOAA, 1966–96: *Climatological Data.* Vols. 70–100.
Pandey, G. R., D. R. Cayan, and K. P. Georgakakos, 1999: Precipitation structure in the Sierra Nevada of California during winter. *J. Geophys. Res.,* **104,** 12 019–12 030.
——, ——, M. D. Dettinger, and K. P. Georgakakos, 2000: A hybrid orographic plus statistical model for downscaling daily precipitation in northern California. *J. Hydrometeor.,* **1,** 491–506.
Rasmussen, L. A., and W. V. Tangborn, 1976: Hydrology of the North Cascades region, Washington 1. Runoff, precipitation, and storage characteristics. *Water Resour. Res.,* **12,** 187–202.
——, H. Conway, and P. S. Hayes, 2001: Estimating Olympic Peninsula precipitation from upper air wind and humidity. *J. Geophys. Res.,* **106,** 1493–1501.
Schermerhorn, V. P., 1967: Relations between topography and annual precipitation in western Oregon and Washington. *Water Resour. Res.,* **3,** 707–711.
Schwartz, B. E., and C. G. Wade, 1993: Considerations for the climatologist using North American radiosonde data. Preprints, *Eighth Symp. on Meteorological Observations and Instrumentation,* Anaheim, CA, Amer. Meteor. Soc., J77–J82.
Sinclair, M. R., D. S. Wratt, R. D. Henderson, and W. R. Gray, 1997: Factors affecting the distribution and spillover of precipitation in the Southern Alps of New Zealand—A case study. *J. Appl. Meteor.,* **36,** 428–442.
Speers, P., 1986: Precipitation analysis and modeling in western Washington state. M.S. thesis, Dept. of Atmospheric Sciences, University of Washington, Seattle, WA, 163 pp.
Steenburgh, W. J., and C. F. Mass, 1996: Interaction of an intense cyclone with coastal orography. *Mon. Wea. Rev.,* **124,** 1329–1352.
Tangborn, W. V., and L. A. Rasmussen, 1976: Hydrology of the North Cascades region, Washington 2. A proposed hydrometeorological streamflow prediction method. *Water Resour. Res.,* **12,** 203–216.
von Storch, H., 1999: On the use of ''inflation'' in statistical downscaling. *J. Climate,* **12,** 3505–3506.
Wade, C. G., and B. E. Schwartz, 1993: Radiosonde humidity observations near saturation. Preprints, *Eighth Symp. on Meteorological Observations and Instrumentation,* Anaheim, CA, Amer. Meteor. Soc., 44–49.
Westrick, K. J., and C. F. Mass, 2001: An evaluation of a high-resolution hydrometeorological modeling system for prediction of a cool-season flood event in a coastal mountainous watershed. *J. Hydrometeor.,* **2,** 161–180.
Widmann, M., and C. S. Bretherton, 2000: Validation of mesoscale precipitation in the NCEP reanalysis using a new gridpoint dataset for the northwestern United States. *J. Climate,* **13,** 1936–1950.
Wilby, R. L., and T. M. L. Wigley, 2000: Precipitation predictors for downscaling: Observed and general circulation model relationships. *Int. J. Climatol.,* **20,** 641–661.
Wilson, L. L., D. P. Lettenmaier, and E. Skyllingstad, 1992: A hierarchical stochastic model of large scale atmospheric circulation patterns and multiple station daily precipitation. *J. Geophys. Res.,* **97,** 2791–2809.
Yang, D., B. E. Goodison, J. R. Metcalfe, V. S. Golubev, R. Bates, T. Pangburn, and C. L. Hanson, 1998: Accuracy of NWS 8″ standard nonrecording precipitation gauge: Results and application of WMO intercomparison. *J. Atmos. Oceanic Technol.,* **15,** 54–68.
Zhai, P., and R. E. Eskridge, 1996: Analyses of inhomogeneities in radiosonde temperature and humidity time series. *J. Climate,* **9,** 884–894.